Journal of Visualization, Vol. 9, No. 2 (2006)137-144

Development of a Pressure Sensitive Paint Technique for Low-Speed Flows and Its Application

Lee, S. J.* and Kang, J. H.*

* Dept. Mech. Eng., Pohang University of Science and Technology, San 31, Hyoja-dong, Pohang 790-784, South Korea. E-mail: sjlee@postech.ac.kr

Received 25 March 2005
Revised 20 December 2005

Abstract : Pressure sensitive paint (PSP) techniques have been used to measure the pressure distribution on a model surface in high-speed flows. In this study, we developed a PSP technique that can be applied to low-speed flows. Four PSP formulations, each comprised of a porphyrin (PtOEP or PtTFPP) and a polymer (Poly(TMSP) or RTV-118), were tested and the performance of each combination was evaluated. In the static calibration, the luminescence intensity of the PSP coatings was measured from 0 kPa to 11 kPa with 0.5, 1, and 2 kPa increments. Among the four PSP formulations tested, the combination of PtOEP and RTV-118 (PSP-3) showed the best performance. In this study, the low-pressure PSP technique using PSP-3 was applied to an oblique impinging subsonic jet to measure pressure field distributions on the impingement plate at various angles of the oblique jet. For comparison, the flow over the impingement plate was visualized using an oil-film method.

Keywords : Pressure sensitive paint (PSP), Oxygen quenching, Low-speed flow, Luminophore, Polymer binder.

1. Introduction

The pressure sensitive paint (PSP) method is an optical pressure measurement technique that measures pressure distributions over the surface of a body by using the theory of oxygen quenching. This method has several advantages over conventional point-wise pressure measurement methods such as pressure tap, pressure transducer, and microphone methods. First, it measures the pressure distribution over the entire surface with a high spatial resolution. Second, it does not require modification of the structure of a model for installing pressure taps, and thus avoids the bias errors that are introduced by such modifications. Third, PSP materials are cheaper than those required for conventional methods. And fourth, PSPs can be used to measure the pressure distributions on surfaces with complex 3-D geometries and on the surfaces of rotating turbomachines such as propellers and fans.

In 1980s, the PSP technique had been regularly applied for measuring surface pressure distribution since its aerodynamic applications were introduced (Peterson et al., 1980; Bukov et al., 1993; Engler et al., 2000). Subsequently, PSP techniques suitable for use in low-speed flows were developed (Brown et al., 1997; Moris et al., 1995; Shimbo et al., 1997; Togerson et al., 1996; Bell, 2004). Recently, many efforts have focused on coating techniques (Asai et al., 1995) and improvement of the PSP formulation for low-speed flow applications (Liu et al., 1997, 2001; Mori et al., 2004). The motivation of this study is to develop a suitable PSP formulation that can be used for

low-speed flows.

In this study, the performance of four PSP formulations comprised of a porphyrin (PtOEP or PtTFPP) and a polymer (Poly(TMSP) or RTV-118) with a high oxygen permeability were tested using a static calibration approach in the low-pressure regime. To verify the practical feasibility of the developed PSPs, the best PSP was used to measure pressure field variations on an impingement plate subjected to an oblique impinging subsonic jet with varying the angle of incidence of the jet. The PSP performance was assessed by comparing the results with those obtained by visualizing the flow structure over the impingement plate using an oil-film method.

2. Background

2.1 Photo-Physical Foundation

The PSP technique is based on the luminescence process in which a luminophore is inactivated by oxygen molecules. When a luminophore absorbs a photon, the energy level rises from the ground state to an exited state. The excited luminophore typically returns to the ground state by emitting a new photon of longer wavelength or by colliding with oxygen molecules without photoemission. The latter process is called oxygen quenching. The oxygen quenching process is proportional to the oxygen concentration. The luminescence intensity depends on the quenching rate of oxygen.

The oxygen quenching process can be described using the Stern-Volmer relation (Parker, 1968), which can be written in the form

$$\frac{I_0}{I} = 1 + k_q \cdot [O_2] \tag{1}$$

where I_0 is the luminescence intensity measured under vacuum, I is the luminescence intensity, k_q is the Stern-Volmer quenching constant of the molecules, and $[O_2]$ is the oxygen concentration. Both I_0 and k_q are functions of the temperature, T. However, this form of the Stern-Volmer relation is difficult to apply to aerodynamic tests directly, because it requires measurement of the luminescence intensity under vacuum conditions.

Equation (1) can be transformed into a form suitable for aerodynamic testing by taking the ratio of the luminescence intensity for two different flows, one with the flow and the other without (McLachlan et al., 1995). This transformation gives

$$\frac{I_{ref}}{I} = A_0(T) + A_1(T)\frac{P}{P_{ref}} \tag{2}$$

where I_{ref} and P_{ref} are the luminescence intensity and pressure for the wind-off condition, respectively, and I and P are the luminescence intensity and pressure for the wind-on condition. Equation (2) indicates that the relative intensity ratio (I_{ref}/I) is linearly proportional to the relative pressure ratio (P/P_{ref}). However, the practical relationship between the intensity and pressure to be measured has nonlinear characteristics for some cases. For this reason, the modified nonlinear Stern-Volmer relation should be considered:

$$\frac{P}{P_{ref}} = \sum_{n=0}^{N} A_n(T)\left(\frac{I_{ref}}{I}\right)^n \tag{3}$$

where the coefficient A_n is the temperature-dependent calibration constant determined from the static calibration. To adequately consider the nonlinear characteristics, a third-order polynomial (N = 3) was used in this study. The temperature dependence of A_n is due to the luminescence quenching of the luminophore and the dependence of the oxygen permeability of the polymer binder on the temperature (Liu et al., 1997).

2.2 PSP Combination

PSPs are usually composed of a luminophore and a polymer binder. The polymer binder is used to adhere the luminophore onto the model surface. In addition, the polymer may significantly affect the photophysical behavior of the paint through complicated interactions between the luminophore and the macromolecules of the polymer (Liu et al., 1997).

In this study, two types of polymer with high oxygen permeability, Poly(TMSP) and RTV-118, were used as the polymer binder. As a luminophore, the organic Pt dyes PtOEP and PtTFPP were tested. Table 1 lists the compositions of the four PSPs tested in this study, which are denoted PSP-1 to -4. The PSPs were applied to an aluminum plate (100 mm × 100 mm × 1 mm) that had first been coated with white paint using an air-brush and then allowed to dry at room temperature. The PSPs were coated onto the painted plate to a thickness of about 10~15 μm using an air-brush. The coating thickness of the PSP layer plus the white paint layer was about 25~30 μm The coating thickness was measured with the coating thickness meter (MEGA-CHECK FN).

Table 1. The composition of PSP tested in this study.

	Luminophore	Polymer binder
PSP-1	PtTFPP	RTV-118
PSP-2	PtTFPP	Poly(TMSP)
PSP-3	PtOEP	RTV-118
PSP-4	PtOEP	Poly(TMSP)

3. Calibration

3.1 Static Calibration

The luminescence intensity of the PSP samples was measured with increasing pressure inside the pressure chamber, which had a clear optical window, at regular pressure intervals. In the static calibration, the coefficients of the Stern-Volmer relation were determined.

Figure 1 shows the experimental set-up of the PSP static calibration. The pressure inside the chamber was monitored using a pressure transducer with a spatial resolution of 10 Pa to maintain a pre-set pressure. A 300 W Xenon lamp (Oriel Model 6137) was used a light source to excite the PSP formulation. To prevent temperature rising due to light illumination, a water filter was installed in front of the Xenon lamp. The emission light passed a band-pass optical filter of λ_i = 420 nm (Melles Griot 03FIV028). To minimize the refraction of the light as it passed through the optical window, the camera and illumination light were installed carefully and the Xenon light was irradiated through a fiber optic cable. To reduce the photodegradation effect of continuous light illumination, the light was controlled using a mechanical shutter attached to the Xenon lamp such that the PSP was irradiated only during image acquisition. The spatial distribution of luminescence intensity emitted from the PSP sample was captured using a 12-bit intensified CCD camera (1280 × 1024 pixels). To obtain only the light emitted from the PSP sample, a band-pass filter of λ_o = 650 nm (Melles Griot 03FIVB014) was installed in front of the CCD camera. The exposure time and repetition rate of the CCD camera were 50 ms and 15 frames per second, respectively. In addition, 70 % gain was preset for the intensified CCD to get good PSP images.

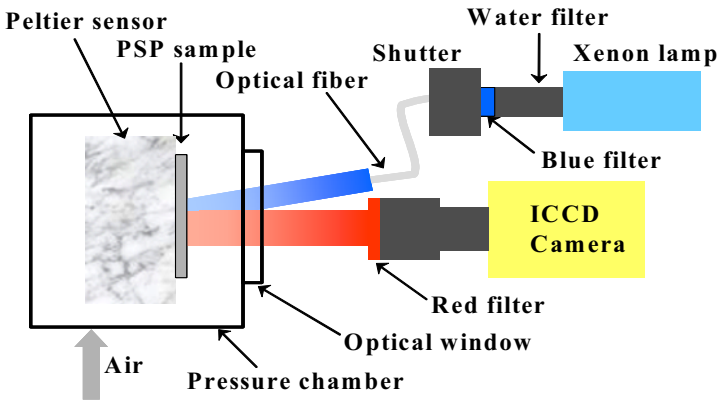

Fig. 1. Schematics of PSP calibration set-up.

3.2 Calibration Results

In the static calibration for the PSP samples, the pressure inside the chamber was increased from 0 kPa to 11 kPa in increments of 0.5, 1, and 2 kPa. The reference pressure P_{ref} was defined as the atmospheric pressure, and the temperature of the tested PSP plates was maintained at T = 24 °C using a Peltier sensor.

For each pressure condition, 120 PSP images were captured and the dark current noise of the CCD camera was removed. The images were then ensemble-averaged to obtain the time-averaged mean pressure distribution. Figure 2 shows the variation of the intensity ratio with respect to the PSP formulation. PSP-1 (Fig. 2(a)) is insensitive to the pressure difference in the low-pressure range. This seems to be attributed to the photochemical interaction between the luminophore and the polymer binder. PSP-3, on the other hand, shows a higher sensitivity and nonlinear relationship in the low-pressure range compared to the other formulations. In particular, the variation rate of intensity ratio was about 40 % of the full intensity range in the low-pressure range (0~2 kPa). To determine the Stern-Volmer coefficients of PSP-3, the least-square curve fitting (N= 3) was applied. Figure 2(b) shows the calibration curve for PSP-3; the four calibration coefficients are A_0 = 110.2, A_1 = 84.911, A_2 = -201.69, and A_3 = 107.88.

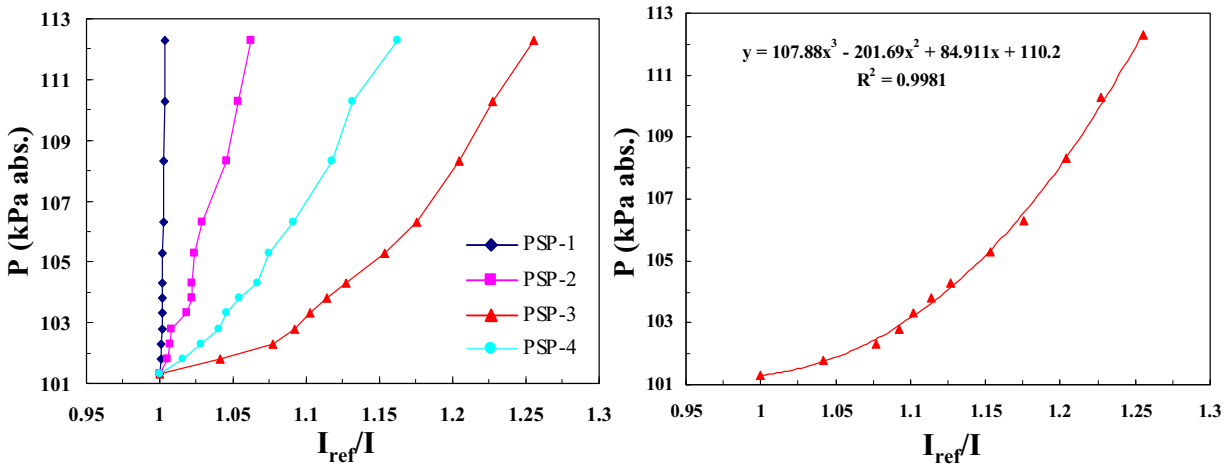

(a) Comparison of luminescence intensity ratio (b) Calibration curve of PSP-3

Fig. 2. Results of static calibration at T = 24 °C.

The effect of temperature on the measured intensity values of PSP-3 formulation was evaluated to be less than 0.72 %/°C. The sensitivity was evaluated to be about 840 % per bar at 101 kPa and 145% per bar at 112 kPa. The large sensitivity at lower pressures is a good merit for PSP measurements of low-speed flows. This may be related with the bimolecular quenching rate and collisional frequency of the PSP formulation. Future study on the proper quenching model to explain the sensitivity variation of the PSP-3 formulation is needed.

4. Application to Oblique Impinging Jet

4.1 Experimental Apparatus

To verify the feasibility and usefulness of the PSP-3 formulation, which showed good sensitivity in the static calibration, the PSP was coated onto the impingement plate of an oblique impinging jet. Figure 3 shows the experimental set-up for measuring the pressure distribution on the impingement plate (Lee et al, 2002). The arrangement of the illumination light source and the CCD camera is the same as for the static calibration. In this study, a simple round-shaped nozzle was used to generate a low-speed jet flow. The nozzle diameter of the impinging jet (D) was 3 mm, and the angle between the nozzle and the impingement plate (θ) was 30°, 50° or 70°. The distance between the jet nozzle and the impingement plate (G) was nondimensionalized by the nozzle diameter. In this study, pressure distributions were measured for a gap distance of $G/D = 1$ and an exit velocity of $U = 80$ m/s. Because the temperature difference between the impingement plate and the plate used for the static calibration was less than ±0.5 °C, thermal effects due to variations in the ambient temperature can be ignored. The temperature of impingement plate was measured using a thermocouple.

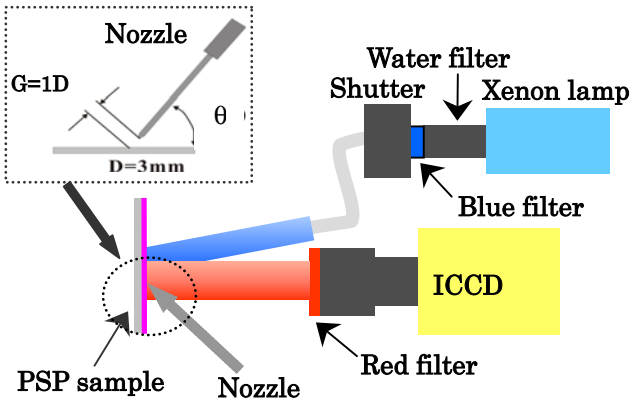

Fig. 3. Experimental set-up for PSP measurements of an oblique impinging jet.

To visualize the surface flow over the impingement plate, the oil film method (Yang, 1989) with a mixture of silicon oil (KF-96-10CS) and fine powder (soots) was employed. Oleic acid was added to the oil suspension to prevent coagulation of the particles. Because the oil suspension was black, the plate was pre-coated with white paint to enable observation of the particles. The oil suspension was painted onto the surface with a brush, and particle trajectories were recorded using a digital camera.

To verify the measurement accuracy of the PSP technique, eleven pressure taps were installed along the center line of impingement plate. The pressure taps were connected to the transducer of Scanivalve (48J9-1, ZOC 23B) system with vinyl tubes of 0.8 mm inner diameter. A high-precision A/D converter (DT2838) was used to digitize the analog voltage output from the pressure transducer as to the engineering unit. For each channel, 10,000 pressure data points were acquired at a sampling rate of 200 Hz. Static pressure values were averaged by getting pressure data five times.

4.2 Results and Discussion

The pressure distributions on the impingement plate were derived using the following image procedure. The dark-current level image was captured with the light source turned off before the main experiment. This image was subtracted from the images acquired in the wind-on and wind-off conditions to remove the dark-current noise of the CCD camera. The intensity ratio (I_{ref}/I) was then determined by dividing the wind-off image intensity (I_{ref}) by the wind-on image intensity (I). Finally, the pressure distribution on the plate was obtained using the Stern-Volmer coefficients derived from the static calibration and Eq. (3).

The mean pressure distribution was obtained by averaging 120 instantaneous pressure distributions obtained from PSP images. Here, the axial direction along which the flow moves on the impingement plate is designated the X axis and the perpendicular direction is defined as the Y axis. As shown in Fig. 4, the maximum pressure increases as the jet angle is increased. The surface pressure has a local maximum at the location where the impinging jet directly strikes the plate. As the jet angle increases, the contours expand in the X-direction but shrink in the Y-direction. This results from the fact that the impingement area where the flow collides with the plate with large momentum increases with decreasing jet angle. For the case of $\theta = 70°$ (Fig. 4(c)), the surface pressure more rapidly decreases with increasing distance from the impingement point, compared with the other cases. This also results from the reduction of the direct collision area of the impinging jet.

Figure 5 shows the visualized flow structure on the impingement plate. The length of the particle trajectories along the axial X-direction is increased and the spreading on the surface is concentrated largely toward the axial direction, as the angle (θ) between the nozzle and plate decreases. For the case of $\theta = 70°$, the outward movement of tracer particles is very weak. The visualization results look similar to the pressure contours of the PSP results, indicating that the PSP technique can be used to visualize the surface flow on a body surface.

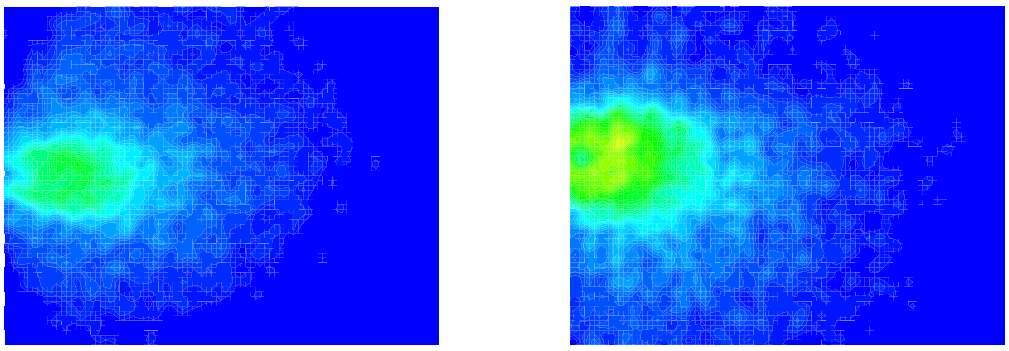

(a) $\theta = 30°$ (b) $\theta = 50°$

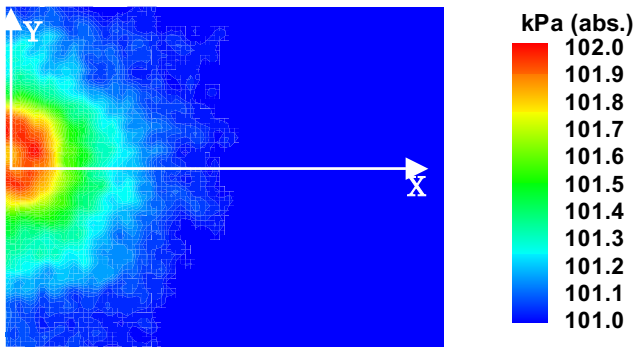

(c) $\theta = 70°$

Fig. 4. Mean pressure distribution on the impingement plate of PSP images with respect to angle variations at $G/D = 1$.

To verify the measurement accuracy of the PSP technique employed in this study, the PSP results were compared with pressure data measured using pressure taps. Figure 6 shows a comparison of the pressure variation along the center line, as measured by the PSP and pressure tap methods. The general patterns of the pressure variations along the centerline for the two methods are similar. On average, the difference between the PSP data and pressure data measured using pressure taps on the model surface is about ±50 Pa. The maximum pressure occurs at X = 3 mm rather than at X = 0 mm. This is attributed to the fact that the jet impinges on the plate at an oblique angle. In the θ = 70° system, the pressure decreases rapidly with going downstream from the stagnation point such that, by about X = 22 mm, the pressure is nearly equal to the atmospheric pressure. For the smaller angles, however, the pressure remains above atmospheric pressure all the way to the end of the test plate.

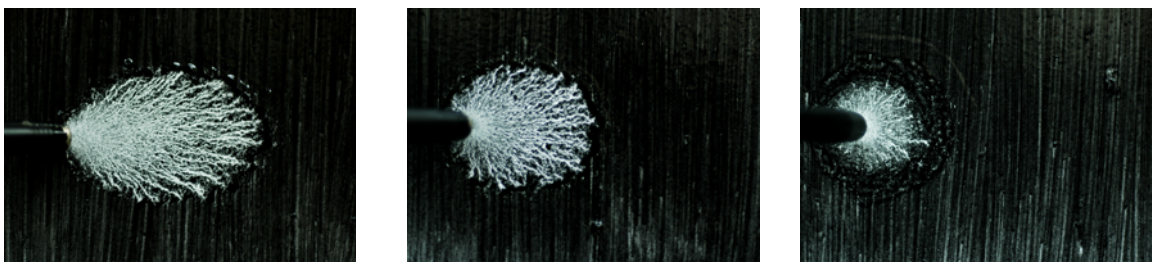

(a) θ = 30° (b) θ = 50° (c) θ = 70°

Fig. 5. Visualized surface flow on the impingement plate at *G/D* = 1.

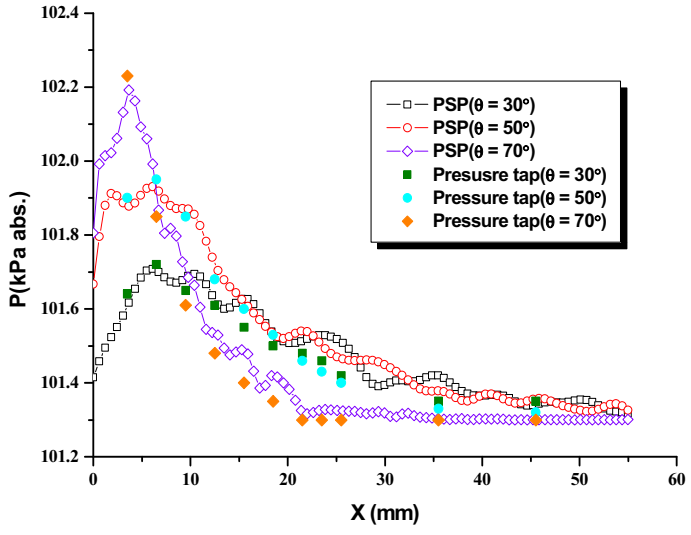

Fig. 6. Pressure variation along the center line with respect to jet angle at *G/D* = 1.

5. Conclusion

The performances of four PSP formulations composed of a porphyrin (PtOEP or PtTFPP) and a polymer (Poly(TMSP) or RTV-118) were tested though static calibration. The reaction characteristics of the PSPs in the low-pressure regime depended not only on the luminophore, but also on the polymer binder and the interaction. Among the four PSP formulations tested, the combination of PtOEP and RTV-118 (PSP-3) showed the best performance in the low-pressure range. When PSP-3 was applied to a low-speed oblique impinging jet to estimate its feasibility and usefulness, the

results obtained were in good agreement with those obtained by the pressure tap method. The pressure field distribution on the impingement plate for the oblique impinging jet was well matched with the visualized flow structure obtained using an oil-film method.

Acknowledgment

The present work is supported by National Research Laboratory Program of Ministry of Science and Technology (MOST) of Korea.

References

Asai, K., Kanda, H. and Iijima, Y., Luminescent Characteristics of Pressure Sensitive Paint Based on Platinum Octaethylporphyrin, The 23rd Symp. on Flow Visualization, (1995).
Bell, J. H., Applications of Pressure-Sensitive Paint to Testing at Very Low Flow Speeds, the 42nd AIAA Aerospace Sciences Meeting and Exhibit (Reno, Nevada), AIAA Paper 2004-087 (2004).
Brown, O. C., Metha, R. D. and Cantwell, B. J., Low-speed Flows Studies Using the Pressure Sensitive Paint Technique, 81st AGARD/FDP, (1997).
Bukov, A., Mosharov, V., Orlov, A., Pesetsky, V., Radchenko, V., Phonov, S., Matyash,S., Kuzmin, M. and Sadozsky, N., Optical Surface Pressure Measurements: Accuracy and Application Field Evaluation, 73rd AGARD Fluid Dynamics Panel Meeting and Symp. on Wall Interference (Brussels, Belgium), (1993), Support Interference and Flow Field Meas.
Engler, R. H., Mrienne, M. C., Klein, C. and Sant, Y. L., Application of PSP in Low Speed Flows, Aerospace Science and Technology, 6-5 (2002), 313-322.
Lee, S. I. and Lee, S. J., Performance Comparison of Pressure Sensitive Paint and Pressure Field Measurement of Oblique Impinging Jet, KSME, 26-7 (2002), 1031-1038.
Liu, T., Campbell, B. T., Burns, S. P. and Sullivan, J. P., Temperature- and Pressure-Sensitive Paint Luminescent Paints in Aerodynamics, Appl. Mech. Rev., 50-4 (1997), 227-246.
Liu, T., Guille, M. and Sullivan, J. P., Accuracy of Pressure Sensitive Paint, AIAA, 39-1 (2001), 103-112.
McLachan, B. G. and Rell, J. H., Pressure Sensitive Paint in Aerodynamic Testing, Exp. Thermal and Fluid Sci., 10 (1995), 470-485.
Moris, M. J., Use of Pressure Sensitive Paint in Low-speed Flows, 16th ICIASF (OH, USA), (1995), USAF Wright Laboratory.
Mori, H, Niimi, T., Yoshida, M., Kondo, M. and Oshima, Y., Application of PSP to Low Density Gas Flow, J. of Visualization, 7-1 (2005), 55-62.
Park, C. A., Photoluminescence of Solutions, (1968), Elsevier Publ., New York.
Torgerson, S. D., Liu, T. and Sullivan, J. P., Use of pressure sensitive paints in low speed flows, AIAA Paper 96-2184 (1996).
Yang, W. J., Handbook of Flow Visualization, (1989), Hemisphere Publ., New York.

Author Profile

Sang Joon Lee: He received his master and Ph.D. in Mechanical Engineering from KAIST in 1982 and 1986, respectively. In 1986 he worked as a senior researcher at KIMM. He has been currently a professor in the Department of Mechanical Engineering at POSTECH from 1987. His research interests are quantitative flow visualization (PIV, PTV, LIF, Holography, X-ray imaging), experimental fluid mechanics, bluff body aerodynamics, microfluidics, and bio-fluid flows.

Jong Hoon Kang: He received his master degree in Mechanical Engineering in 2004 from POSTECH. He is a Ph.D student at POSTECH and his research interests are PSP technique and wind engineering.